

Depth-resolved fluorescence spectroscopy of normal and dysplastic cervical tissue

Yicong Wu, Peng Xi and Jianan Y. Qu

Department of Electrical and Electronic Engineering, Hong Kong University of Science and Technology, Clear Water Bay, N.T., Hong Kong SAR, P. R. China
eequ@ust.hk

Tak-Hong Cheung and Mei-Yung Yu

Department of Obstetrics and Gynecology, Chinese University of Hong Kong, Prince of Wales Hospital, Shatin, N.T., Hong Kong SAR, P. R. China

Abstract: A portable confocal system with the excitations at 355nm and 457nm was instrumented to investigate the depth-resolved fluorescence of cervical tissue. The study focused on extracting biochemical and morphological information carried in the depth-resolved signals measured from the normal squamous epithelial tissue and squamous intraepithelial lesions. Strong keratin fluorescence with the spectral characteristics similar to collagen were observed from the topmost keratinizing layer of all tissue samples. It was found that NADH and FAD fluorescence measured from the underlying non-keratinizing epithelial layer were strongly correlated to the tissue pathology. This study demonstrates that the depth-resolved fluorescence spectroscopy can potentially provide more accurate diagnostic information for determining tissue pathology.

©2005 Optical Society of America

OCIS codes: (170.6510) Spectroscopy, tissue diagnostics.

References and Links

1. N. Ramanujam, M. F. Mitchell, A. Mahadevan, S. Warren, S. Thomsen, E. Silva and R. Richards-Kortum, "In vivo diagnosis of cervical intraepithelial neoplasia using 377-nm-excited laser-induced fluorescence," *Proc. Natl. Acad. Sci. USA*, **91**, 10193-10197 (1994)
2. S. K. Chang, M. Follen, A. Malpica, U. Utzinger, G. Staerckel, D. Cox, E. N. Atkinson, C. MacAulay and R. Richards-Kortum, "Optimal excitation wavelengths for discrimination of cervical neoplasia," *IEEE Trans. Biomed. Eng.* **49**, 1102-1110 (2002)
3. R. Drezek, C. Brookner, I. Pavlova, I. Boiko, A. Malpica, R. Lotan, M. Follen and R. Richards-Kortum, "Autofluorescence microscopy of fresh cervical-tissue sections reveals alterations in tissue biochemistry with dysplasia," *Photochem. Photobiol.* **73**, 636-641 (2001)
4. I. Pavlova, K. Sokolov K, R. Drezek, A. Malpica, M. Follen and R. Richards-Kortum, "Microanatomical and biochemical origins of normal and precancerous cervical autofluorescence using laser-scanning fluorescence confocal microscopy," *Photochem. Photobiol.* **77**, 550-555 (2003)
5. Y. Wu, P. Xi, J. Y. Qu, T. Cheung and M. Yu, "Depth-resolved fluorescence spectroscopy reveals layered structure of tissue," *Opt. Express* **12**, 3218-3223 (2004)
<http://www.opticsexpress.org.ezproxy.ust.hk/abstract.cfm?URI=OPEX-12-14-3218>
6. M. G. Muller, T. A. Valdez, I. Georgakoudi, V. Backman, C. Fuentes, S. Kabani, N. Laver, Z. Wang, C. W. Boone, R. R. Dasari, S. M. Shapshay, M. S. Feld, "Spectroscopic detection and evaluation of morphologic and biochemical changes in early human oral carcinoma," *Cancer* **97**, 1681-169 (2003)
7. B. Chance, B. Schoener, R. Oshino, F. Itshak, and Y. Nakase, "Oxidation-reduction ratio studies of mitochondria in freeze-trapped samples," *J. Biol. Chem.* **254**, 4764-4771 (1979)
8. G. M. Palmer, C. L. Marshak, K. M. Vrotsos and N. Ramanujam, "Optimal methods for fluorescence and diffuse reflectance measurements of tissue biopsy samples," *Lasers Surg. Med.* **30**, 191-200 (2002)
9. T. Collier, D. Arifler, A. Malpica, M. Follen and R. Richards-Kortum, "Determination of Epithelial tissue scattering coefficient using confocal microscopy," *IEEE. J. Sel. Top. Quantum Electron.* **9**, 307-313(2003)
10. C. Carrilho, M. Alberto, L. Buane and L. David, "Keratins 8, 10, 13, and 17 are useful markers in the diagnosis of human cervix carcinomas," *Hum. Pathol.* **35**, 546-551(2004)

1. Introduction

Autofluorescence spectroscopy has the potential to effectively and noninvasively probe biochemical and biomorphological alterations in precancerous tissue. Clinical investigations have demonstrated that fluorescence spectra obtained from the normal and dysplastic cervical tissue exhibited inherent differences [1,2]. A variety of diagnostic algorithms were developed to classify the fluorescence signals and differentiate cervical intraepithelial neoplasia (CIN) from normal cervical tissue based on the spectral differences. The study using the cervical tissue samples cultured from biopsies revealed an increase in NADH fluorescence and a decrease in redox ratio in the dysplastic epithelium, which indicated an increased metabolic activity [3,4]. Furthermore, a decrease in stromal fluorescence, attributed primarily to changes in the collagen biochemistry, was observed in dysplastic tissue.

A clear understanding of the biological basis of autofluorescence provides insight valuable to improving the diagnostic performance of fluorescence spectroscopy. Recently, we developed a confocal spectroscopy system to study the depth-resolved autofluorescence of biological tissue samples. It was found that keratin produces strong collagen-like fluorescence in the topmost layer of squamous epithelium [5]. The keratin signal creates interference for the assessments of NADH/FAD fluorescence in the epithelium and collagen fluorescence in the stroma. In this work, we investigate the depth-resolved autofluorescence of fresh cervical tissue samples using a portable confocal fluorescence spectroscopy system. The primary goal is to develop further understanding on biochemical and biomorphological mechanisms responsible for the fluorescence characteristics of normal and precancerous cervical tissue.

2. Materials and methods

A portable confocal system equipped with two compact lasers of wavelengths at 355 nm and 457 nm was instrumented. The collimated UV and blue laser beams were combined with a dichroic mirror. Two lasers shared the same optical path to excite the fluorescence from tissue sample and the corresponding fluorescence signals were collected by a single optical fiber as the confocal pinhole. The axial and lateral resolutions of the system were about 3 μm and 1.8 μm , respectively. The method to collect high-quality depth-resolved autofluorescence signal was the same as that used in the previous work [5]. Autofluorescence with a high signal-to-noise ratio (SNR) was recorded when the power of UV and blue laser on tissue sample were controlled at 20 μW and 50 μW , respectively. No photobleaching was observed.

Fresh ectocervical specimens covered with squamous epithelial cells were obtained from the anterior and posterior cervix of a group of patients undergoing the loop electrosurgical excision procedure (LEEP). All the samples were rinsed briefly with PBS solution to remove the residual blood on the surfaces. Two stitches were made at the 3 o'clock and 9 o'clock positions in each sample to define a line across the sample. The depth-resolved measurements were conducted in two or three sites along the line at an interval of 3 mm, starting at the site about 6 mm away from the stitch located at 3 o'clock position. The number of measurement sites in each sample was dependent on the size of samples. The sample preparation and fluorescence measurements were completed within 40 minutes after LEEP. Tissue samples were fixed with formalin for histological analyses after the fluorescence measurements. Histological sections were made with the tissue slices cut from the sites where depth-resolved fluorescence were measured. The tissue slices were perpendicular to the fluorescence measurement line defined by the stitches.

3. Results and discussion

A total of 18 ectocervical tissue samples were obtained from 12 patients enrolled in this study. Maximally one sample was excised from anterior and posterior cervix of each patient, respectively. The patient's age was in the range from 21 to 47 years (mean age 36 ± 7). The sample size was from 12-15 mm along the measurement line defined by the stitches. Depth-resolved fluorescence spectra were recorded from 39 tissue sites of 18 samples. The histopathological analysis showed that 14 examined sites were normal, 10 sites exhibited HPV

infection and 15 sites had developed to CIN at different grades (4 CIN I, 4 CIN II, 7 CIN III). The depth-resolved measurements from two extremes, a sample with highly keratinizing epithelium and a sample with lightly keratinizing epithelium, are shown in Figs. 1(a-d) as the representative results. The spectra shown in Figs. 1(a) and 1(c) and Figs. 1(b) and 1(d) were excited by the 355 nm and 457 nm laser, respectively. Each spectrum is normalized to its peak intensity. The inset of each figure shows the peak intensity of raw fluorescence signals measured at different depths. The depth of 0 μ m refers to the tissue surface where the confocal signal of reflection from the interface between the tissue and the glass coverslip reaches to maximum.

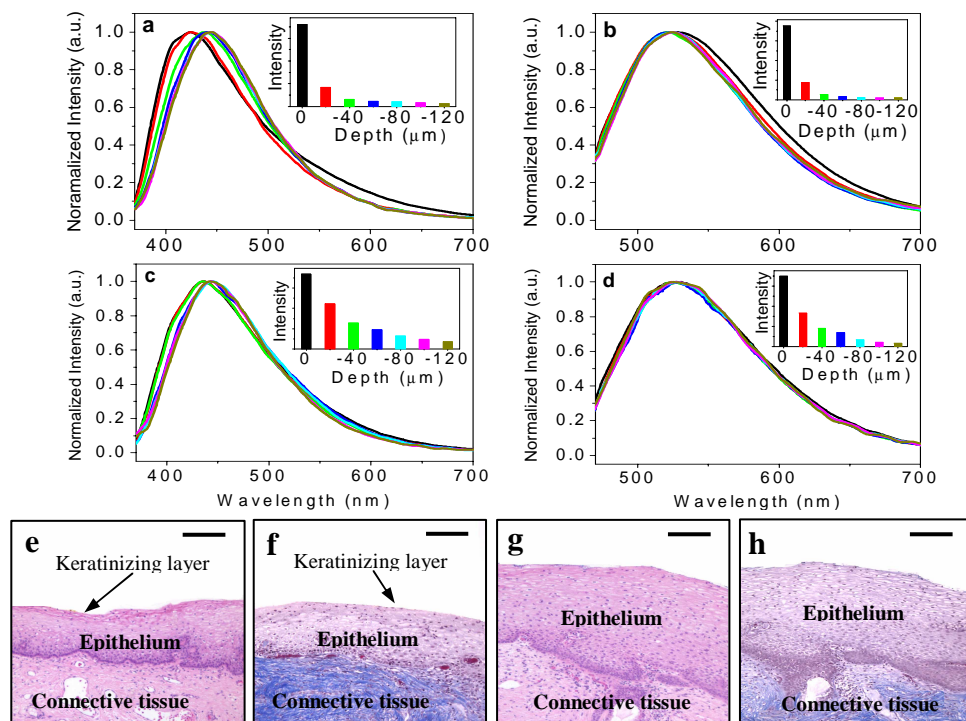


Fig. 1. Representative depth-resolved autofluorescence signals of ectocervical tissue and corresponding histology. a (209kB), b: spectra recorded from a sample with highly keratinizing epithelium; c (250kB), d: spectra recorded from a sample with lightly keratinizing epithelium; e, f: corresponding H&E- and Mason-stained sections of the sample with highly keratinizing epithelium; g, h: corresponding H&E- and Mason-stained sections of the sample with lightly keratinizing epithelium; Scale bar in the histology e-h: 100 μ m.

The animation of Fig. 1(a) displays the fluorescence spectral signal as a function of depth. Strong fluorescence peaked at 420 nm from the tissue surface to the depth of 30 μ m show the dominance of the keratin signal with the spectral characteristics similar to collagen [5]. The fluorescence spectra measured at the depths from 40 μ m to 120 μ m, the maximal detection depth of current system, are all peaked at 440 nm, the emission peak of NADH fluorescence signal. This indicates that NADH is the dominant fluorophore in the underlying epithelium. The signals measured in the transition zone at the depths of 30-40 μ m are the mixture of NADH and keratin fluorescence. The H&E-stained histology in Fig. 1(e) shows clearly the keratinizing structure in the topmost layer of thickness about 30 μ m. The Mason-stained section coloring collagen into blue is displayed in Fig. 1(f). It provides the evidence that the collagen are distributed in the stroma under the epithelium. The fluorescence in the topmost keratinizing layer are contributed from the keratin and not linked with the collagen network. Thus, the information extracted from the depth-resolved fluorescence reveals fine layered structure of the epithelium that are consistent with the histological analyses.

Figure 1(b) displays the fluorescence spectra measured from the same sample using a 457 nm laser that mainly excited keratin and FAD fluorescence. The signals at different depths are almost peaked at 530 nm because FAD fluorescence can not be well distinguished from keratin fluorescence using a 457 nm excitation [5].

The depth-resolved fluorescence signals measured from a sample with lightly keratinizing epithelium are displayed in Figs. 1(c) and 1(d). The animation of Fig. 1(c) shows that the fluorescence measured from the topmost layer of the thickness about 50 μm is a mixture of keratin fluorescence and NADH fluorescence. The NADH fluorescence peaked at 440 nm becomes dominant from the depths of 60 μm to 120 μm . Though the information derived from the depth-resolved measurements show that the topmost lightly keratinizing epithelium is about 50 μm thick, it is almost histologically invisible from the standard H&E-stained histology in Fig. 1(g). This suggests that the depth-resolved fluorescence spectroscopy is more sensitive in sensing the keratinization of tissue than standard histological analysis. The Mason-stained section shown in Fig. 1(h) confirms no collagen in the epithelium. Fig. 1(d) displays the spectra excited at 457 nm. All the signals are peaked at 530 nm that are similar to the results measured from the sample with highly keratinizing epithelium in Fig. 1(b).

In general, the depth-resolved fluorescence spectra from 39 measurement sites of 18 ectocervical tissue samples demonstrate that the cervical squamous epithelium has layered structure. This is consistent with the study of the squamous epithelial tissue of animal models [5]. With a 355nm excitation, the fluorescence peak of the topmost layer varies in the range from 420nm to 435nm, which shows the mixture of keratin and NADH signals and reflects the degree of keratinization of the epithelial tissue. Starting from a certain depth, the fluorescence peak is red-shifted to $440\pm 3\text{nm}$, the emission peak of NADH. With a 457 nm excitation, the emission peaks at different depths are always at $530\pm 3\text{nm}$. The depth-resolved measurements show that the thickness of the keratinizing layer is in the range from 20-50 μm . It was found that the degree of keratinization and thickness of the keratinizing layer vary from measurement site-to-site and do not have obvious correlation with the tissue pathology. The fluorescence from the highly keratinizing layer are dominated by the keratin signal and are a factor of 3-6 stronger than the NADH/FAD signals from the underlying epithelial layer. However, the axial gradient of the fluorescence is much smaller in the sample with lightly keratinizing epithelium as shown in Figs. 1(c) and 1(d). This may be due that the content of keratin is high in the highly keratinizing layer and the keratinized structure scatters the excitation light and reduces its penetration into deeper layer [6].

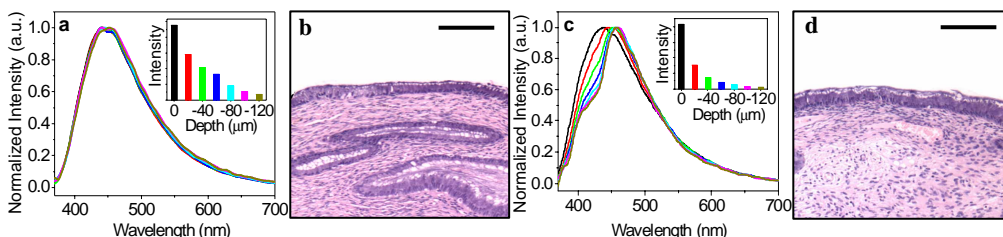


Fig. 2. Depth-resolved fluorescence spectra and corresponding histology of endocervical tissue samples. a, b: spectra and histology of a sample with normal submucosa; c, d: spectra and histology of a sample with highly vascularized submucosa. Scale bar in histology: 100 μm .

Cervix consists of two parts, the ecto- and endo-cervix that are covered with squamous and columnar epithelium, respectively. The two kinds of epithelial tissues are formed with different cells. To explore whether the cervical tissue is generally keratinized, the depth-resolved measurements were performed on two normal endocervical tissue samples obtained from the hysterectomy surgeries. The depth-resolved fluorescence excited at 355 nm and the histology of the endocervical samples are displayed in Fig. 2. The histology of the samples in Figs. 2(b) and 2(d) show the layered structure of endocervical tissue in which the submucosa is covered with the columnar epithelium of thickness about 30 μm . However, the layered structure is not revealed in the depth-resolved spectra measured from a sample with normal

submucosa as shown in Fig. 2(a). The fluorescence spectra at different depths are almost identical and peaked at 440 nm, the peak wavelength of NADH fluorescence, which means that NADH is the dominant fluorophore in both columnar epithelium and submucosa. The keratin fluorescence signal was not found in the epithelial layer. Figs. 2(c) and 2(d) display the depth-resolved spectra and histology of a sample with highly vascularized submucosa. The epithelial fluorescence is still dominated by the NADH signal. The lineshape of the fluorescence signal from the submucosa is obviously modulated by the strong absorption of blood in the wavelength region from 400-430 nm. The measurements from both samples also indicate that collagen is not a major contributor to the fluorescence of endocervical tissue.

The depth-resolved fluorescence spectroscopy of cervical squamous epithelial tissue has revealed that keratin is a major fluorophore in the topmost keratinizing layer. The fluorescence from underlying non-keratinized epithelium are determined by the signals of NADH and FAD, the coenzymes related to cellular metabolism, when excited by a 355 nm and a 457 nm source, respectively. To investigate the possible correlation between the epithelial fluorescence and tissue pathology, we calculated the averaged peak intensity of the depth-resolved fluorescence spectra recorded from all the tissue sites grouped as normal, HPV infection and CIN (CIN I, CIN II, CIN III). The results are displayed in Fig. 3. As can be seen, the axial gradient of the fluorescence in the topmost 40 μm layer is significantly greater than that in the underlying layer. The relative intensity of the groups of normal, HPV infection and CIN remains almost same in the topmost keratinizing layer regardless the tissue pathology. However, the averaged intensity of the fluorescence excited at 355nm increases in the CIN group comparing to the normal group starting from the depth of 50 μm to 120 μm as shown in Fig. 3(a). In addition, the averaged intensity of the fluorescence excited at 457nm decreases in the CIN group comparing to the normal group in the same depth range as shown in Fig. 3(b). This indicates that NADH fluorescence increase and FAD fluorescence decrease in the dysplastic cervical tissue, which is consistent with the study on short-term cervical tissue culture [3,4]. Quantitatively, about 50% increase of NADH fluorescence and 40% decrease of FAD fluorescence were found in CIN tissue by integrating the averaged fluorescence intensity over the depth from 50 to 120 μm .

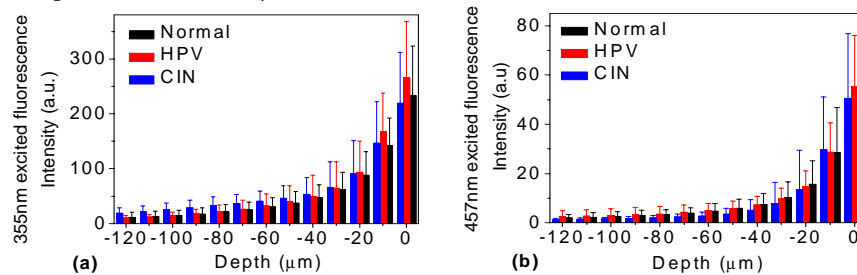


Fig. 3. The averaged fluorescence intensities of the groups of normal tissue, HPV infection and CIN; a: 355nm excitation; b: 457nm excitation. Error bars represent standard deviations.

In principle, the metabolic rate of tissue can be evaluated by calculating the redox ratio defined as the absolute FAD fluorescence over the sum of absolute FAD and NADH fluorescence [3]. However, the fluorescence excitation cross-sections of NADH and FAD in the intracellular fluid are unknown. It is difficult to obtain an accurate redox ratio in tissue independent on measurement system. Here, we calculate the ratio of the UV laser excited NADH fluorescence at 440-450 nm over the blue laser excited FAD at 525-535 nm and investigate the correlation between the ratio and tissue pathology. This UV/Blue ratio should reflect the status of tissue metabolism because NADH is an electron donor and FAD is an electron acceptor in the cellular metabolic process [7]. The UV/Blue ratio as a function of depth calculated from the spectra recorded from each measurement site are shown in Fig. 4(a). Again, the results are grouped into normal, HPV and CIN. In the topmost layer of 40 μm thickness, the ratio values of CIN group are at the same level as normal and HPV group, which shows no correlation between the ratio and tissue pathology because of the

dominance/interference of the keratin fluorescence. However, in deeper layer with the ending of keratinization in epithelium, the ratio values of the CIN group become significantly higher than normal and HPV groups. It was found that the mean ratio in CIN group increased about 2.4 times while the ratio of normal and HPV groups remain almost unchanged. The Student's t-test was used to evaluate the statistical difference in the UV/Blue ratio value between the normal/HPV groups and CIN group. The p-values of the Student's t-test as a function of depths are shown in Fig. 4(b). As can be seen, p-values become much smaller than 0.01 when the detection depth is over 50 μ m, which indicates that the difference in UV/Blue ratio between the normal/HPV groups and CIN group is statistically significant. The UV/Blue ratio is highly correlated to the tissue pathology. It should be emphasized that although most of sites in CIN group can be clearly differentiated from the normal group based on the UV/Blue ratio, there are about 20% sites in CIN and normal groups produce the ratio values overlapping to each other. It may be due to the error in identifying the measurement sites to make tissue section for histological analysis and the possible degradation of tissue samples over the time frame after the LEEP [8].

The scattering is a dominant factor to determine the propagation of light in the epithelial tissue. A significantly increased scattering has been observed in high-grade CIN [9]. With first-order approximation of Beer's law, the confocal signal decays exponentially according to the scattering coefficient. The UV/Blue ratio is a function of tissue scattering properties. An increased scattering in high-grade CIN may cause an underestimation of metabolic rate in the epithelial tissue that is proportional to the ratio of intrinsic NADH signal over FAD signal.

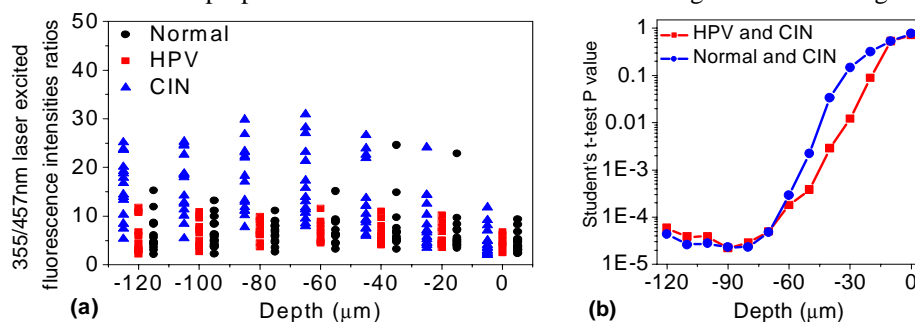


Fig. 4. (a) Scatter plot for the UV/Blue ratio of each measurement site as a function of depth; (b) p-value of student's t-test of normal and HPV vs. CIN groups as a function of depth.

4. Conclusion

We demonstrate that the depth-resolved fluorescence spectroscopy can provide important biochemical and morphological information on epithelial tissue where most of precancers originated. The cervical squamous epithelium is generally more or less keratinized. Under the excitation at 355 nm and 457 nm, keratin fluorescence in the topmost keratinizing layer with 20-50 μ m thickness cause interference in seeking the correlation between the fluorescence and tissue pathology. The depth-resolved fluorescence technique can effectively reduce the interference and isolate the NADH and FAD signals from the underlying non-keratinized epithelial layer. The ratio of NADH over FAD fluorescence measured in the non-keratinized epithelium is strongly correlated to tissue pathology. These results provide profound insight into the biological basis of the inherent differences in fluorescence of normal and dysplastic ectocervical tissue. The future study will focus on developing a miniaturized confocal probe to conduct the depth-resolved fluorescence measurement at clinical level. In addition, the depth-resolved fluorescence method is a sensitive technique to detecting keratin that comprises over 20 intermediate filament proteins. The possible correlation between keratin signal excited at other wavelengths and the tissue pathology will be explored because a recent study showed that keratin expression patterns could be used as the natural biomarkers for diagnosis of human cervix carcinoma [10]. Also, the effect of keratinization of epithelial tissue on the measurements of NADH over FAD fluorescence will be investigated. This study

was supported by the Hong Kong Research Grants Council through grants HKUST6052/00M and HKUST6025/02M.